

## Surface transfer doping of hydrogen-terminated diamond by C60F48: Energy level scheme and doping efficiency

M. T. Edmonds, M. Wanke, A. Tadich, H. M. Vulling, K. J. Rietwyk, P. L. Sharp, C. B. Stark, Y. Smets, A. Schenk, Q.-H. Wu, L. Ley, and C. I. Pakes

Citation: *The Journal of Chemical Physics* **136**, 124701 (2012); doi: 10.1063/1.3695643

View online: <http://dx.doi.org/10.1063/1.3695643>

View Table of Contents: <http://scitation.aip.org/content/aip/journal/jcp/136/12?ver=pdfcov>

Published by the [AIP Publishing](#)

---



## Re-register for Table of Content Alerts

Create a profile.



Sign up today!



# Surface transfer doping of hydrogen-terminated diamond by C<sub>60</sub>F<sub>48</sub>: Energy level scheme and doping efficiency

M. T. Edmonds,<sup>1,a)</sup> M. Wanke,<sup>2</sup> A. Tadich,<sup>1,3</sup> H. M. Vulling,<sup>1</sup> K. J. Rietwyk,<sup>1</sup> P. L. Sharp,<sup>4</sup> C. B. Stark,<sup>1</sup> Y. Smets,<sup>1</sup> A. Schenk,<sup>1</sup> Q.-H. Wu,<sup>1</sup> L. Ley,<sup>1,2</sup> and C. I. Pakes<sup>1</sup>

<sup>1</sup>Department of Physics, La Trobe University, Victoria 3086, Australia

<sup>2</sup>Institut für Technische Physik, Universität Erlangen, Erwin-Rommel-str. 1, 91058 Erlangen, Germany

<sup>3</sup>Australian Synchrotron, 800 Blackburn Road, Clayton, Victoria 3168, Australia

<sup>4</sup>School of Physics and Astronomy, University of Nottingham, Nottingham NG7 2RD, United Kingdom

(Received 22 November 2011; accepted 4 March 2012; published online 23 March 2012)

Surface sensitive C1s core level photoelectron spectroscopy was used to examine the electronic properties of C<sub>60</sub>F<sub>48</sub> molecules on the C(100):H surface. An upward band bending of 0.74 eV in response to surface transfer doping by fluorofullerene molecules is measured. Two distinct molecular charge states of C<sub>60</sub>F<sub>48</sub> are identified and their relative concentration determined as a function of coverage. One corresponds to ionized molecules that participate in surface charge transfer and the other to neutral molecules that do not. The position of the lowest unoccupied molecular orbital of neutral C<sub>60</sub>F<sub>48</sub> which is the relevant acceptor level for transfer doping lies initially 0.6 eV below the valence band maximum and shifts upwards in the course of transfer doping by up to 0.43 eV due to a doping induced surface dipole. This upward shift in conjunction with the band bending determines the occupation of the acceptor level and limits the ultimately achievable hole concentration with C<sub>60</sub>F<sub>48</sub> as a surface acceptor to values close to 10<sup>13</sup> cm<sup>-2</sup> as reported in the literature. © 2012 American Institute of Physics. [<http://dx.doi.org/10.1063/1.3695643>]

## I. INTRODUCTION

Diamond with a bandgap of 5.47 eV is an insulating material when undoped. However, the diamond surface exhibits interesting functional properties when terminated with hydrogen. The C–H bond at the terminated surface creates a dipole layer which induces a negative electron affinity (EA) of up to –1.3 eV and lowers the ionization potential from 5.8 eV to as low as 4.2 eV, lower than that of any known semiconductor.<sup>1</sup> As a consequence, electron transfer from the valence band of diamond into the lowest unoccupied molecular orbital (LUMO) of an appropriate adsorbate is possible, thereby providing a mechanism for the formation of a sub-surface hole accumulation layer. The surface transfer doping model was used by Maier *et al.* to explain successfully the formation of *p*-type surface conductivity (SC) when the H-terminated diamond surface is exposed to ambient conditions. Here, the doping relies on the electrochemical redox reaction between a thin adsorbed water layer and the diamond surface.<sup>2</sup> Strobel *et al.* demonstrated that *p*-type surface doping of diamond could also be achieved with fullerene (C<sub>60</sub>) and fluorofullerenes (FFs, C<sub>60</sub>F<sub>x</sub>, x = 18, 36, 48) as surface acceptors where doping is achieved by the transfer of an electron to the LUMO of C<sub>60</sub>F<sub>x</sub>.<sup>3,4</sup> The introduction of the strongly electronegative fluorine atoms induces a large electron affinity in the fluorofullerenes, allowing an electron-hole pair for each C<sub>60</sub>F<sub>x</sub> acceptor and hence a doping efficiency of one because the activation energy is initially negative. However, the doping efficiency drops to zero above a critical FF coverage and that limits the ultimate hole concentration and

thus achievable surface conductivity. The hole concentration at saturation differs for the different FFs and appears to scale with the electron affinity of the FF; with  $p \sim 10^{13}$  cm<sup>-2</sup> at its highest for C<sub>60</sub>F<sub>48</sub> which in vapour form has an EA of 4.06 eV, higher than any of the other FFs.<sup>5</sup> Significant progress has been made in characterising the electronic properties of the diamond surface and the underlying two-dimensional hole accumulation layer.<sup>6–9</sup>

Air-induced *p*-type SC on diamond has led to the development of metal-semiconductor field effect transistors (FET),<sup>10</sup> and more recently solution gated FET (Ref. 11) that utilise this surface accumulation layer. The development of devices using molecules as surface acceptors is in its infancy by comparison. However, there is a potentially wide choice of molecular systems with properties that can be systematically modified to introduce functional properties in addition to being acceptors. While the response of diamond to surface transfer doping has been extensively studied, little attention has been paid to the properties of the surface molecules on H-terminated diamond and the effect of charge transfer on their energy level structure. Knowledge of the electronic behaviour of the molecular acceptors is of fundamental importance to understanding, for example, the limitations to achieving higher hole sheet densities in the underlying *p*-type layer and to the selection and design of alternative molecular acceptors.

In this paper we specifically address the question of what factors determine the ultimate achievable hole concentration, or in other words, what makes the doping efficiency drop to zero above a certain acceptor coverage and how does that depend on the electronic level scheme of acceptor molecules and diamond. The acceptor we use is C<sub>60</sub>F<sub>48</sub> on C(100):H

<sup>a)</sup>Electronic email: mtedmonds@students.latrobe.edu.au.

and the main investigation tool is core-level photoelectron spectroscopy (PES) using synchrotron radiation. The surface sensitivity of this technique, combined with high energy resolution, permits for the first time the identification of two distinct  $C_{60}F_{48}$  charge states, corresponding to ionized and neutral fluorofullerene molecules. An increase in the energy of the LUMO of the neutral  $C_{60}F_{48}$ , arising from an induced potential at the diamond-fluorofullerene interface, limits the maximum achievable hole sheet density whereupon further deposited fluorofullerenes no longer participate in surface transfer doping.

## II. EXPERIMENTAL DETAILS

Experiments were performed using a boron-doped (100) single crystal synthetic IIb diamond sample with a boron concentration of  $5 \times 10^{18}$  to  $5 \times 10^{19} \text{ cm}^{-3}$ .<sup>12</sup> Using the energy of the boron acceptor (373 meV) and the boron concentration, the Fermi level position in the bulk is calculated to lie between 0.19 and 0.21 eV above the valence band maximum (VBM). The sample was cleaned by boiling in acid ( $H_2SO_4/HClO_4/HNO_3$ ; 1:1:1) in order to remove metallic contamination and non-diamond carbon phases. Hydrogen termination was performed in microwave hydrogen plasma at a sample temperature of 800 °C for 45 min. The sample was exposed to air before being transferred to ultra-high vacuum ( $10^{-10}$  mbar) at the soft x-ray beamline of the Australian Synchrotron, where subsequent processing and PES measurements were performed. The sample was annealed *in vacuo* to 550 °C for 1 h prior to PES measurements to remove airborne hydrocarbon contamination and any air-induced surface conductivity without impairing the hydrogen termination.

$C1s$  core level spectra were measured with an overall energy resolution of  $\sim 0.1$  eV at normal emission using a photon energy  $\hbar\omega = 330$  eV in order to maximize surface sensitivity. At this photon energy the kinetic energy of the  $C1s$  photoelectrons is about 45 eV, i.e., at the minimum of the electron escape depth. The binding energy (BE) scale is referenced to the Fermi energy  $E_F$  by setting the BE of the  $4f_{7/2}$  core level of a gold (Au) sample in electrical contact with the diamond to a value of 84.00 eV.  $C_{60}F_{48}$  adlayers were deposited by sublimation from a quartz crucible and using a quartz-crystal monitor as a guide to deposition rate.  $C_{60}F_{48}$  coverage was accurately determined from the  $C1s$  spectra using the method adopted by Strobel *et al.* by assuming that for  $\hbar\omega = 330$  eV the mean free path of the  $C1s$  photoelectrons is 3.5 Å.<sup>4</sup> A coverage of one monolayer (ML) corresponds to  $7.80 \times 10^{13} \text{ C}_{60}F_{48} \text{ molecules/cm}^2$ . Photoemission measurements were performed on the pristine C(100):H surface and with  $C_{60}F_{48}$  coverages ranging from 0.002 ML to 1 ML. Experiments determining the extent of damage to  $C_{60}F_{48}$  arising from exposure to synchrotron radiation have been reported by us in Ref. 13. For extended beam exposure  $C_{60}F_{48}$  dissociates by a flux of secondary electrons from the underlying diamond and the released F atoms lead to the formation of a fluorine-terminated surface by replacing C–H with C–F bonds. In the present study each  $C1s$  core-level spectrum took 150 s to collect and a different region of the surface was analysed for each coverage to minimise dissociation. After the spectra for

a particular coverage were taken, the sample was annealed at 350 °C for 30 min to remove the irradiated adlayer prior to a subsequent deposition.

After subtracting a background using the Shirley method<sup>14</sup> the  $C1s$  spectra were fitted with a Voigt function where the Lorentz width  $\Gamma_L$  was fixed at 0.15 eV to reflect the lifetime of the  $C1s$  core hole.<sup>15</sup> Shifts in  $E_F$  at the surface were determined with an uncertainty of  $\pm 0.02$  eV by the measured shift in the diamond bulk component. By using the fixed energy separation of the VBM to the  $C1s$  core level of  $283.9 \pm 0.1$  eV as reported by Maier *et al.* the position of  $E_F$  relative to  $E_{VBM}$  has been determined.<sup>16</sup> The change in Fermi level position so obtained was corrected to account for the convolution of the  $C1s$  line with the band profile at high hole sheet densities as reported by us in Ref. 17. The highest correction amounts to 0.10 eV.

## III. RESULTS

Figure 1 gives a series of  $C1s$  spectra together with the fitted components for: (a) clean H-terminated diamond and (b)–(f) increasing  $C_{60}F_{48}$  coverage. There are two distinct groups of  $C1s$  lines. The group around 284 eV binding energy stems from bulk diamond and the C–H and C–H<sub>x</sub> surface entities that are chemically shifted to higher binding energies by 0.25 eV and 0.58 eV, respectively. The position of the C–H peak and its identification is presented in Ref. 18. The wide group between 286 and 290 eV is due to carbon atoms in the fluorinated fullerenes. The spectral region at lower binding energy, labelled C=C, is due to carbon atoms surrounded by carbon only, whereas the higher BE region represents carbon atoms that have one fluorine (F) atom attached to them; the two regions are separated by  $2.07 \text{ eV} \pm 0.05 \text{ eV}$ . The binding energies of the diamond bulk and fluorofullerene line components and their relative intensities are listed in Table I for the spectra shown in Fig. 1. For coverages of 0.088 ML and above the C=C and C–F lines require two distinct components for a proper fit (labelled C=C, (C=C)<sup>−</sup> and C–F, (C–F)<sup>−</sup>, respectively, in Fig. 1). That indicates the presence of two distinct molecular charge states, the origin of which will be discussed below. At coverages exceeding 0.503 ML additional components with low intensity (labelled C=C<sub>x</sub> and C–F<sub>x</sub>) are included and arise from the dissociation of fluorine for cases where the fluorofullerene coverage is high. These lines need not concern us here and play no part in the following discussion.

## IV. DISCUSSION

### A. Surface band bending

The variation in  $E_F - E_{VBM}$  at the surface as a function of  $C_{60}F_{48}$  coverage is shown in Fig. 2. Starting from a position slightly above the bulk Fermi level position (0.4 vs. 0.2 eV)  $E_F$  moves rapidly towards  $E_{VBM}$  and drops below  $E_{VBM}$  for coverages in excess of about 0.02 ML. This is equivalent to a corresponding upward band bending and a clear sign of the formation of the hole accumulation layer at the diamond surface. A maximum shift in  $E_F$  of 0.74 eV is observed at 0.503 ML coverage. At this point  $E_F$  resides 0.35 eV below

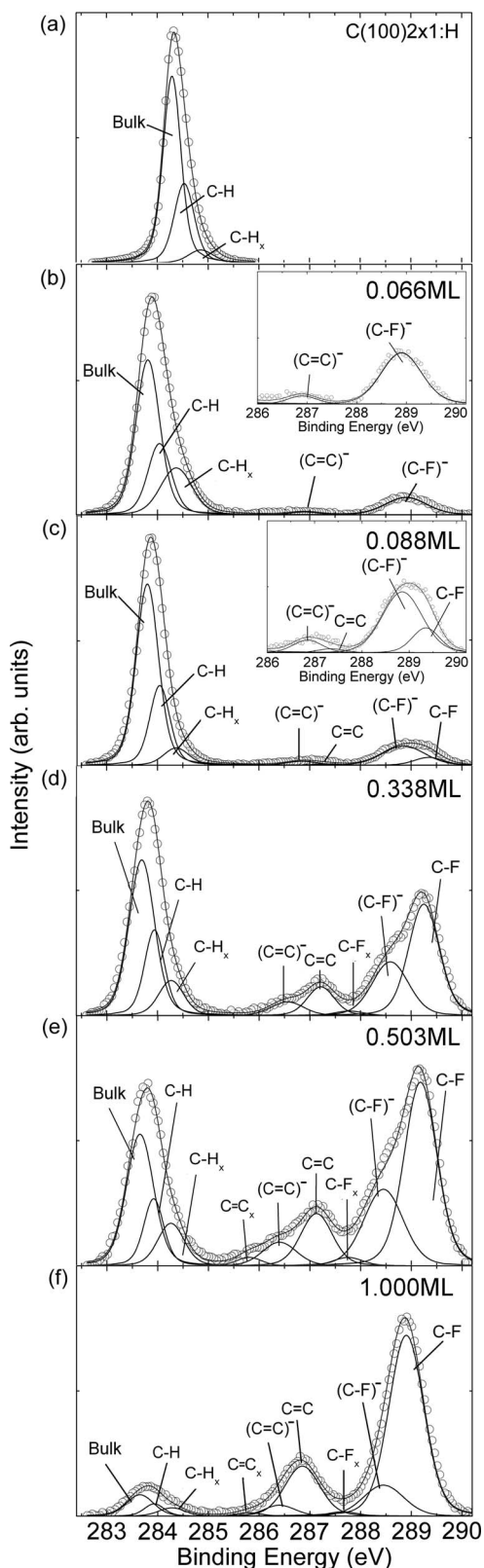


FIG. 1.  $C1s$  spectra taken at 330 eV for: (a) clean H-terminated diamond and (b)–(f) selected  $C_{60}F_{48}$  coverage between 0.066 ML and 1.0 ML.

the VBM whereupon the Fermi level no longer changes for further  $C_{60}F_{48}$  deposition. At low coverage, the Fermi level shift in response to  $C_{60}F_{48}$  deposition follows the same trend as reported in Refs. 17 and 19, with the final position of  $E_F - E_{VBM}$  around  $\sim 0.2$  eV higher than previously measured.

## B. Identification of neutral and ionized fluorofullerene molecules

Turning now to the  $C1s$  spectra of the fluorofullerenes shown in Fig. 1, the remarkable aspect is the fact that both the  $C=C$  and  $C-F$  groups consist of two distinct components clearly separated in binding energy by about 0.6 eV and whose relative intensities are the same in both spectral regions. In other words, there appear to be two chemically different groups of  $C_{60}F_{48}$  molecules on the surface of hydrogen-terminated diamond. These we interpret as neutral (A) and ionized ( $A^-$ )  $C_{60}F_{48}$  acceptors with concentrations  $N_A$  and  $N_{A^-}$ , respectively. The  $C1s$  lines at lower binding energy correspond to the ionized fluorofullerenes because the extra charge lowers all binding energies on account of the additional Coulomb repulsion. This interpretation is confirmed by studying the  $C=C$  and  $C-F$  groups of  $C_{60}F_{48}$  molecules on the oxygen-terminated diamond surface as shown in Fig. 3. Oxygen-terminated diamond has a large positive electron affinity<sup>16</sup> that prevents surface transfer doping, meaning that only neutral  $C_{60}F_{48}$  molecules will be present on the oxygen-terminated diamond surface. This is shown in Fig. 3 where only one component is needed to fit the  $C=C$  and  $C-F$  groups, confirming our interpretation of ionized and neutral  $C_{60}F_{48}$  molecules on the hydrogen-terminated diamond surface.

Figure 4 shows the fractional concentration of the ionized  $C_{60}F_{48}$ . It is evident that at low coverage  $N_{A^-}$  dominates and at high coverage  $N_A$ . The changeover point occurs between 0.1 ML and 0.3 ML. That suggests that what we see in Fig. 4 is the changeover from mainly ionized  $C_{60}F_{48}$ , i.e., doping molecules below 0.1 ML to an increasing contribution of non-doping neutral  $C_{60}F_{48}$  for higher coverages. Above 0.5 ML, further deposited  $C_{60}F_{48}$  no longer participates in surface transfer doping. This interpretation is in accord with that of Strobel *et al.* who observed a saturation in the fluorofullerene induced hole concentration at about 0.2 ML.<sup>4</sup> The difference in binding energy of the two species is listed in Table I and is seen to remain constant at  $0.58 \pm 0.07$  eV. There is some scatter in the difference depending on coverage but not in a way that lends itself to further interpretation. We shall focus now on the  $C1s$  energies of the doping component in the  $C=C$  part of the spectrum (the  $(C=C)^-$  component) because it is well defined in all spectra and all other components are linked to it by constant energy differences.

When we turn to the variation in the  $C1s$  binding energies of the doping  $(C=C)^-$  component, the intention is to learn something about the level alignment between diamond and the doping fluorofullerenes as a function of coverage. The aim is to understand the factors that limit the ultimate hole concentration obtained by surface transfer doping diamond with fluorofullerene. The underlying assumption is that the relevant LUMO level maintains a constant energy separation from the  $C=C$  core level much as the justified assumption of a fixed energy separation between the VBM and  $C1s$  core level in diamond enabled us to extract the surface band bending from the variation in the diamond  $C1s$  energy relative to  $E_F$  with fluorofullerene coverage.



TABLE I. Binding energy and relative intensity of the line components for selected  $C_{60}F_{48}$  coverages.

$C_{60}F_{48}$ coverage	Pristine	0.002 ML	0.066 ML	0.088 ML	0.338 ML	0.503 ML	1.000 ML
<b>Diamond bulk</b>							
Position	284.29 eV	284.02 eV	283.81 eV	283.80 eV	283.69 eV	283.65 eV	283.65 eV
Area	214.577	194.093	114.166	135.173	54.496	35.138	9.202
<b>C=C (ionized)</b>							
Position	...	287.30 eV	286.90 eV	286.85 eV	286.56 eV	286.4 eV	286.4 eV
Area	...	...	2.489	4.074	6.029	7.748	5.363
<b>C=C (neutral)</b>							
Position	...	...	...	287.35 eV	287.22 eV	287.13 eV	286.85 eV
Area	...	...	...	1.200	10.676	15.945	27.058
<b>C-F (ionized)</b>							
Position	...	289.40 eV	288.90 eV	288.85 eV	288.59 eV	288.45 eV	288.45 eV
Area	...	1.242	21.018	25.946	25.909	28.586	19.238
<b>C-F (neutral)</b>							
Position	...	...	...	289.35 eV	289.25 eV	289.18 eV	288.9 eV
Area	...	...	...	7.509	46.057	58.083	97.700

In principal, there are two possibilities discussed in the literature for the alignment of substrate and overlayer levels involving organic molecules. One is Fermi level alignment and the other is the pinning of the adlayer molecular orbitals to a fixed energy relative to the energies of the substrate.<sup>20,21</sup> For the case of a metal both schemes would give the same result because the Fermi level in a metal is fixed relative to all other metal energies. For semiconductors or insulators as in the case at hand the situation is quite different. The Fermi level is not fixed relative to the energy levels of the semiconductor such as the VBM and conduction band minimum due to doping and band bending as we have seen above. Therefore, in order to decide which situation holds in the present case we have plotted, as a function of coverage, the BE of the doping  $(C=C)^-$  component relative to  $E_F$  and also relative to  $E_{VBM}$  in Fig. 5. The binding energies relative to  $E_F$  are taken directly from fits to the measured spectra as given in

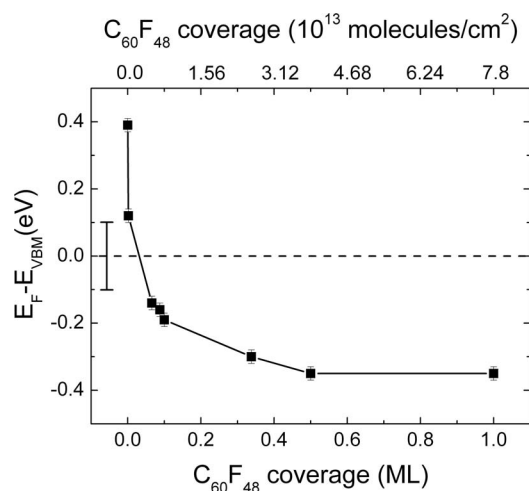


FIG. 2. Surface band bending ( $E_F - E_{VBM}$ ) as a function of  $C_{60}F_{48}$  coverage. The data points contain correction to the  $C1s$  binding energy as described in the text. The error bars on the data points give the uncertainties in the measured Fermi level shift; the large error bar on the dashed line reflects the systematic uncertainty in the  $E_{VBM} - E_{C1s}$  separation.

Table I. By subtracting  $E_F - E_{VBM}$  (see Fig. 2) from these energies the  $(C=C)^-$  doping binding energies relative to  $E_{VBM}$  are obtained as well. It is evident from Fig. 5 that the  $(C=C)^-$  binding energy of the doping molecules is neither constant relative to the Fermi level nor the VBM. By implication, that also holds for the  $LUMO^-$  which is the ionised acceptor level whereas we are really interested in the acceptor level, i.e., the neutral  $LUMO$ . From Table I we know that the separation between the  $C1s$  core levels (and hence the  $LUMOs$ ) of the anion and the neutral molecule is fixed and amounts to 0.58 eV. For a discussion of the variation in  $C=C$  or  $LUMO$  energy

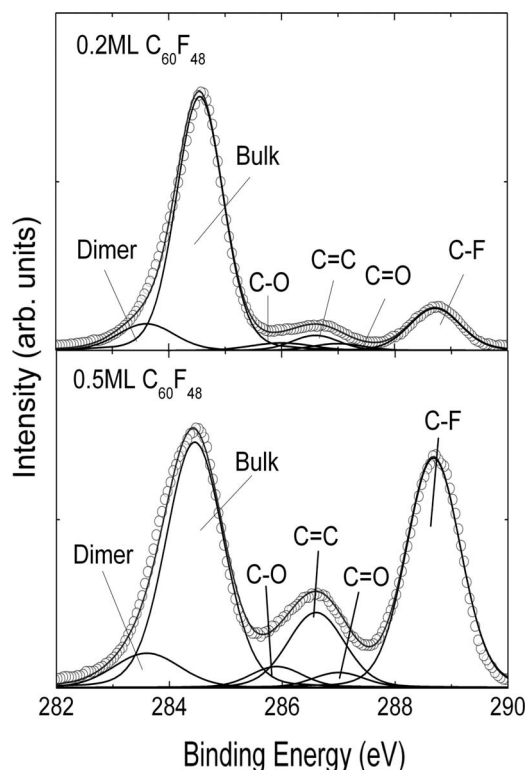


FIG. 3.  $C1s$  spectra taken at 330 eV for O-terminated diamond with 0.2 ML and 0.5 ML  $C_{60}F_{48}$  coverages.

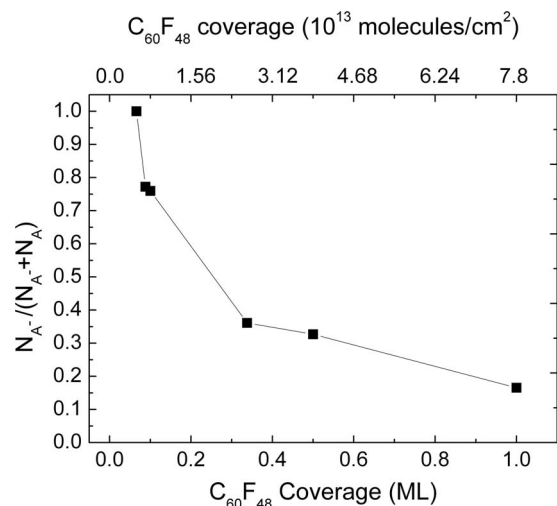


FIG. 4. Relative intensities as a function of coverage of the two components: doping ( $N_{A-}$ ) and non-doping ( $N_A$ ) that make up the C=C and C-F spectral regions of the C1s spectrum of C<sub>60</sub>F<sub>48</sub> on diamond.

we correct the energies of the doping molecules by 0.58 eV. This circuitous way is chosen because for low coverages we do not have reliable values for the non-doping C=C binding energies.

With this approach we plot as squares in Fig. 6  $\Delta$ , the change in the LUMO energy of the neutral fluorofullerenes relative to  $E_{VBM}$  as a function of C<sub>60</sub>F<sub>48</sub> coverage. In analogy to the conventional doping in bulk semiconductors we refer to  $\Delta$  as the acceptor energy. The initial value is  $\Delta_0 = (E_{LUMO} - E_{VBM})$  in the limit of vanishing coverage. From the data it is apparent that our analysis yields an increase in the acceptor energy of 0.19 eV after 0.1 ML coverage and a maximum change of 0.43 eV at 0.5 ML after which  $\Delta$  remains constant as a function of coverage. This means that the acceptor energy is now 0.43 eV higher than the initial value.

What is the origin of this substantial increase in the acceptor energy with increasing fluorofullerene coverage? In a recent publication, we have shown that surface transfer dop-

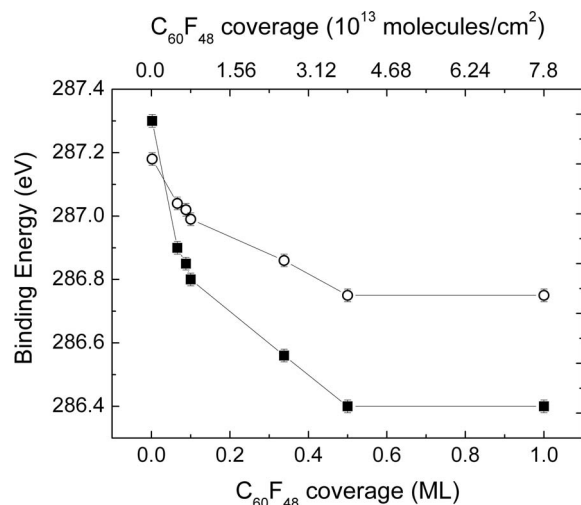


FIG. 5. Binding energy of the (C=C)<sup>-</sup> doping line as a function of C<sub>60</sub>F<sub>48</sub> coverage. Closed squares: relative to  $E_F$  and open circles: relative to the VBM of diamond.

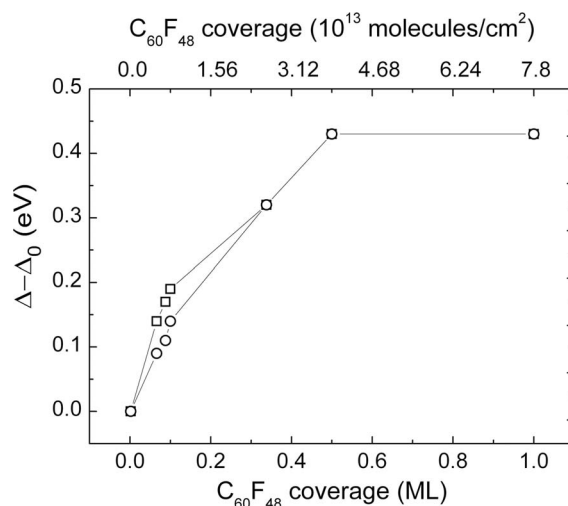


FIG. 6. The increase in acceptor energy  $\Delta = E_{LUMO} - E_{VBM}$  relative to the initial value  $\Delta_0$  as a function of coverage (open squares). Also plotted is the variation in interface potential  $\Delta\Phi$  as calculated in the capacitor model (open circles).

ing with C<sub>60</sub>F<sub>48</sub> is accompanied by a change in EA of diamond of up to 0.63 eV.<sup>17</sup> The origin of this increase in EA lies in the dipole layer that forms between diamond and the acceptor layer at the surface. In the course of transfer doping, electrons are transferred from the diamond into surface acceptors, leaving an equal number of holes behind. The holes are localized in the subsurface accumulation layer in diamond and the electrons are separated from them by the distance of closest approach between diamond and the centre of the charge distribution in the acceptor layer. Connected with the formation of the dipole layer is a potential drop,  $\Delta\Phi$ , that in its most simple form is evaluated by the capacitor model  $\Delta\Phi = ep/C_{\square}$ , where  $p$  and  $C_{\square}$  are the areal charge density and the capacitance of the charge-free region per unit area, respectively, and  $e$  is the elementary charge. With this simple model the variation in EA with carrier concentration could be well accounted for by adopting a specific capacitance  $C_{\square} = 3.25 \times 10^{13} \text{ ecm}^{-2} \text{ V}^{-1}$ .<sup>19</sup>

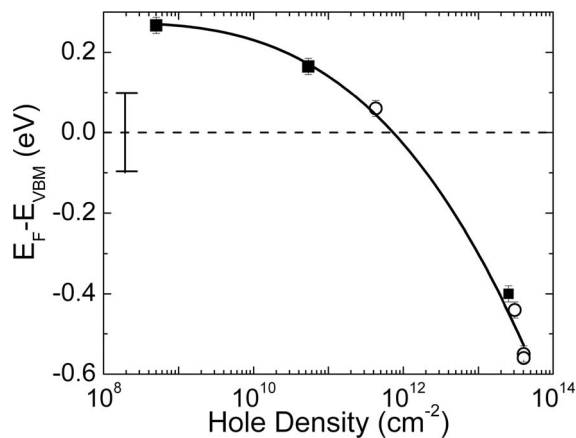


FIG. 7.  $E_F - E_{VBM}$  as a function of hole sheet density for atmosphere (closed squares) and C<sub>60</sub>F<sub>48</sub> (open circles) surface conductivity taken from the work of Edmonds *et al.*<sup>17</sup> The solid line is a polynomial fit of the data to obtain the function  $w(p)$ .

In the present case, the hole sheet density can be determined from the position of  $E_F - E_{VBM}$  in the present work (Fig. 2) by comparison with our previous experimental data of  $E_F - E_{VBM}$  as a function of hole density as shown in Fig. 7.<sup>17</sup> In order to facilitate the comparison we have fitted a polynomial  $w(p)$  to the data as shown by the line in Fig. 7. From the hole sheet densities estimated in this way and the value for the capacitance, the change in potential associated with the dipole layer is plotted as circles in Fig. 6. Taking into account that these data points are derived using experimental input from two different sources, the agreement with the LUMO shift is excellent. The overall amplitude and the general shape in the LUMO shift are matched well by the model. Above 0.5 ML both the potential drop and the acceptor energy no longer change. This is, of course, due to the fact that the doping efficiency of  $C_{60}F_{48}$  is initially equal to one with every fluorofullerene contributing one electron-hole pair. Above about 0.4 ML coverage the relative contribution of non-doping FF dominates and the increase in the dipole levels off as does the surface conductivity. Hence, the maximum possible hole concentration and therefore surface conductivity is determined by a self-limiting process. As more and more charge is transferred the acceptor energy  $\Delta = E_{LUMO} - E_{VBM}$  increases by an amount that itself is linearly related to the charge density. The two acceptor-specific quantities that ultimately determine the achievable hole density for a given temperature are the initial acceptor energy  $\Delta_0$  and the areal capacitance  $C_{\square}$  of the charge-free region separating holes and electrons.

### C. Doping efficiency and initial activation energy $\Delta_0$

As has been pointed out in the original work on transfer doping of diamond by Strobel *et al.*<sup>3,4</sup> doping by fullerenes is governed by Fermi-Dirac statistics and charge neutrality. Hence, the areal hole density  $p$  and the areal density of negatively charged  $C_{60}F_{48}$  molecules are equal and the occupation of the acceptor molecules with one extra electron is given by the Fermi-Dirac probability:

$$\frac{1}{\frac{1}{g} \exp[(E_a)/k_B T] + 1} = \frac{1}{\frac{1}{g} \exp[(E_{LUMO} - E_F)/k_B T] + 1} \quad (1)$$

with  $E_a$  being the activation energy for charge transfer. Following Strobel *et al.* we write the activation energy

$$E_{LUMO} - E_F = \Delta - w(p) = E_{LUMO} - E_{VBM} - (E_F - E_{VBM}). \quad (2)$$

The acceptor energy  $\Delta$  is itself doping dependent and can be further reduced with the result discussed above in connection with Fig. 6:

$$\Delta(p) = \Delta_0 + \Delta\Phi(p) = \Delta_0 + e \cdot p/C_{\square} \quad (3)$$

This yields, for the areal concentration of negatively charged acceptor molecules  $N_{A^-}$ ,

$$N_{A^-} = (N_{A^-} + N_A) \times \frac{1}{\frac{1}{g} \exp[(\Delta_0 + e \cdot p/C_{\square} - w(p))/k_B T] + 1}, \quad (4)$$

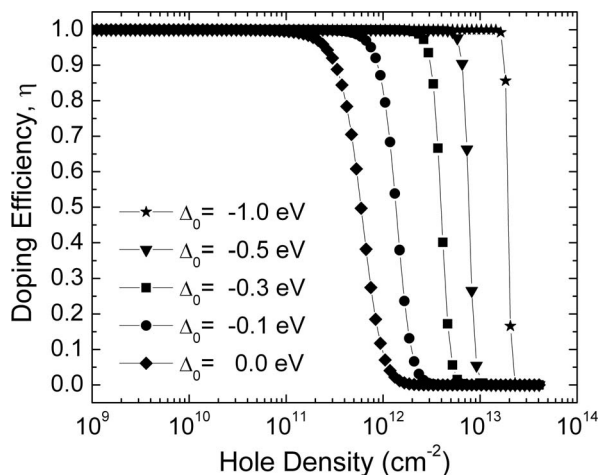


FIG. 8. Doping efficiency as a function of hole density for initial activation energies  $\Delta_0$  ranging from 0 eV to -1 eV.

where  $\Delta_0$  refers to the acceptor energy before any charge transfer has taken place, and  $g = 6$  is the degeneracy factor of the  $C_{60}F_{48}$  LUMO.<sup>4</sup>

Before evaluating Eq. (4) we have to consider the universal (for diamond) function  $w(p)$ . In the work of Strobel *et al.*  $w(p)$  was taken from the theoretical work of Ristein who calculated  $w(p)$  classically.<sup>22</sup> Here, we use  $w(p)$  as derived from experimental data,  $\Delta\Phi(p)$  from the capacitor model, and calculate the doping efficiency  $\eta = N_{A^-}/(N_{A^-} + N_A)$  with  $\Delta_0$  as the only free parameter. This is done in Fig. 8 for  $\Delta_0 = -1.0, -0.5, -0.3, -0.1,$  and  $0$  eV. We see a doping efficiency equal to one below a threshold hole concentration that depends on  $\Delta_0$ ; the lower  $\Delta_0$ , the higher the hole concentration up to which the doping efficiency is unity. This latter regime corresponds to the linear relationship between hole concentration and  $C_{60}F_{48}$  coverage seen in all measurements.<sup>4</sup> At the threshold concentration the doping efficiency drops steeply to zero corresponding to a hole concentration that no longer increases with fluorofullerene coverage. It is clear from Fig. 8 that our model describes quantitatively the relationship between fluorofullerene coverage and hole concentration. Moreover, it gives convincing evidence for the reason why in different experiments different saturated hole densities are observed.

Let us now determine a value for  $\Delta_0$  in the present experiment. Figure 9 plots the experimentally determined and theoretically derived hole densities as a function of  $C_{60}F_{48}$  coverage. The circles represent the hole sheet density determined using the values of  $E_F - E_{VBM}$  in Fig. 2 and the band bending function  $w(p)$ . The squares are derived by making use of the relative intensities of the fluorofullerene core level components to determine the number of doping  $C_{60}F_{48}$  molecules at each coverage, noting that each ionized molecule induces an underlying hole in the diamond. Overall the agreement between these two independently derived hole sheet densities is as good as can be expected. The dashed and solid lines in Fig. 9 correspond to the hole density calculated using Eq. (4) with an initial energy of  $\Delta_0 = -0.5$  and  $-0.7$  eV, respectively. The experimental data fall in between the two estimates and the acceptor energy in the limit of vanishing

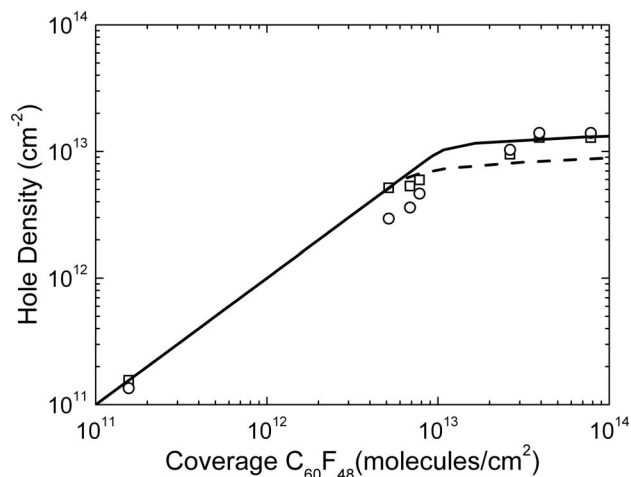


FIG. 9. Experimentally and theoretically determined hole density as a function of  $C_{60}F_{48}$  coverage. Open circles represent the hole sheet density determined using the values of  $E_F - E_{VBM}$  in Fig. 2 and the band bending function  $w(p)$ . Open squares represent the number of doping  $C_{60}F_{48}$  molecules at each coverage calculated from the relative intensities of the fluorofullerene core level components. The dashed and solid lines correspond to the hole density calculated using Eq. (4) with initial activation energies of  $-0.5$  eV and  $-0.7$  eV, respectively.

coverage  $\Delta_0 = (E_{LUMO} - E_{VBM})_{\rightarrow \text{zero coverage}} = -(0.6 \pm 0.1)$  eV for the present experiment.

It is important to recognise that in this case  $\Delta_0$  is not equivalent to the band offset in a conventional semiconductor hetero junction as determined by the bulk properties (charge neutrality levels) of the two adjacent semiconductors, where it solely governs the extent of charge transfer across the interface. Here we are dealing with a molecule only weakly interacting with diamond. Hence, the relevant reference level for level alignment is the vacuum level, which for diamond can change significantly with the degree of hydrogenation. For a perfectly hydrogen terminated surface the EA is  $-1.3$  eV, whereas values closer to  $-1$  eV have frequently been reported that are listed in the work of Maier *et al.*<sup>16</sup>

#### D. Energy level schemes for $C_{60}F_{48}$ on diamond

Finally, we are now in a position to draw the energy level schemes for  $C_{60}F_{48}$  on diamond. This is done in Fig. 10 for the two extreme cases: (a) in the limit of vanishingly small coverage and (b) a coverage of  $\sim 1$  ML where the saturation in hole density and therefore surface conductivity is achieved. In doing so we tacitly assume that the constant separation between LUMO and LUMO<sup>-</sup> prevails down to coverages where spectroscopically no neutral FFs are observed. Using the initial acceptor energy determined in Fig. 9 of  $\Delta_0 = -0.6$  eV, the only energy not measured in the present work is the electron affinity of the pristine hydrogen terminated diamond surface of  $-1.1$  eV taken from our previous work.<sup>19</sup>

Let us, finally, compare some salient energies as they arise from our analysis with literature values. From the bandgap energy of diamond of  $5.47$  eV in conjunction with the electron affinity of diamond and initial acceptor energy we can determine a value for the electron affinity of neutral  $C_{60}F_{48}$ . The electron affinity of the neutral  $C_{60}F_{48}$

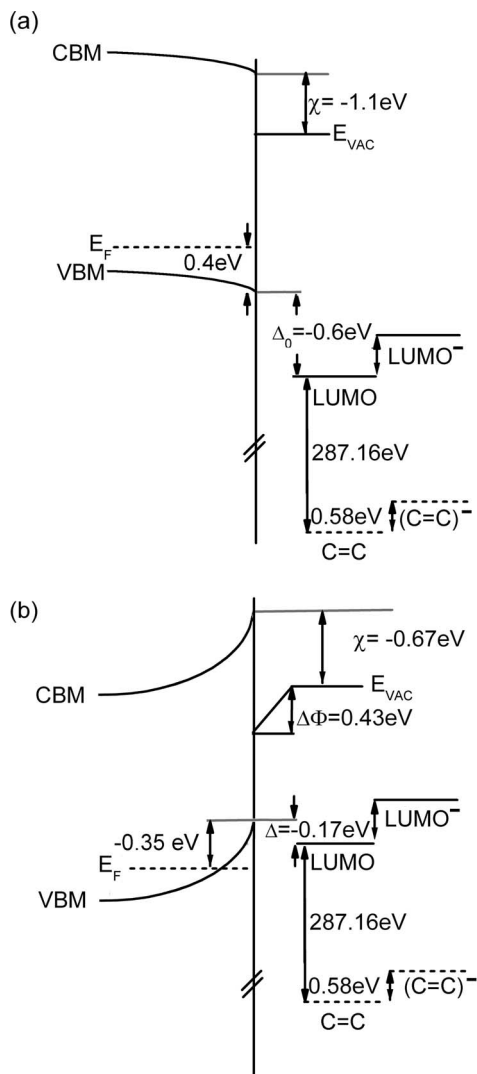


FIG. 10. Band diagram for  $C_{60}F_{48}$  on diamond: (a) in the limit of vanishing concentration and (b) 1 ML  $C_{60}F_{48}$  coverage.

molecules is given by  $\chi_{C_{60}F_{48}} = I - \Delta_0$ , where  $\Delta_0 = -(0.6 \pm 0.1)$  eV from Fig. 9. Assuming  $\chi_{DIAMOND} = -1.1$  eV with a  $\pm 0.2$  eV variance, the electron affinity of neutral  $C_{60}F_{48}$  is  $4.97 \pm 0.2$  eV. Previously reported values are  $4.06$  eV quoted by Jin *et al.* for gaseous  $C_{60}F_{48}$  and  $5.0$  eV reported by Mitsumoto *et al.* for solid  $C_{60}F_{48}$ .<sup>5,23</sup> The difference of  $0.9$  eV between the two reported values is due to screening effects in the solid  $C_{60}F_{48}$ . The value derived by Mitsumoto relied on the assumption that the polarization energy of an electron in  $C_{60}F_{48}$  is the same as in  $C_{60}$  and amounts to  $0.95$  eV.<sup>24</sup> In comparing our result with these two previously reported results, it appears that our result is consistent with that of solid  $C_{60}F_{48}$ . This suggests that the  $C_{60}F_{48}$  core levels are screened from the underlying diamond just as well as from neighbouring FF molecules in the molecular solid.

The other quantity derived by us is the  $E_{LUMO} - E_{C1s}$  separation of  $287.16$  eV  $\pm 0.1$  eV for the C=C component of the C1s spectra. Mitsumoto *et al.* measure a binding energy relative to  $E_F$  of  $286.2$  eV in solid  $C_{60}F_{48}$ , they quote a Fermi level given as  $0.4$  eV below the LUMO which yields  $E_{LUMO} - E_{C1s} = 286.6$  eV, falling short of our value by  $0.56$  eV.<sup>23</sup> In



another paper, Mitsumoto *et al.* report a Fermi level 0.8 eV below the LUMO and the same C1s binding energy, which would reduce the difference between their and our value to 0.16 eV.<sup>25</sup> Given that the analysis of Mitsumoto used the same polarization energy for an electron in C<sub>60</sub>F<sub>48</sub> as in the case of C<sub>60</sub>, and the inherent uncertainties in the present study, the agreement is quite reasonable.

## V. CONCLUSION

By utilizing high resolution, surface sensitive C1s core level photoelectron spectroscopy we have unravelled details in the energy level scheme of diamond and a C<sub>60</sub>F<sub>48</sub> acceptor layer that are crucial for a detailed understanding of the doping mechanism, its efficiency, and the factors that determine the ultimate hole concentration achievable with this acceptor system. Unlike conventional bulk doping in semiconductors, in transfer doping the surface acceptors are no longer characterized by a single acceptor energy, i.e., a single energy difference between acceptor level (the LUMO of C<sub>60</sub>F<sub>48</sub> in our case) and the VBM of diamond. Instead, the acceptor energy is itself a function of doping. This comes about from the dipole layer that forms between the spatially separated holes in diamond and electrons in the acceptor layer. This sets up a dipole potential difference  $\Delta\Phi(p)$  that effectively increases the acceptor energy. The magnitude of the potential difference scales linearly with the amount of transferred charge and the proportionality factor is the inverse of the capacitance of the charge free region between electrons and holes. This capacitance therefore constitutes a system specific quantity that enters in the doping efficiency and the maximum hole density. In the case at hand the capacitance amounts to  $C_{\square} = 3.25 \times 10^{13} \text{ ecm}^{-2}\text{V}^{-1}$  and a maximum change in potential of +0.43 eV.

The other system specific quantity is the acceptor energy  $\Delta_0$  in the limit of vanishing surface acceptor coverage. It amounts to -0.6 eV in our case and the fact that it is negative is responsible for the high initial doping efficiency of one. If one were to treat the diamond-C<sub>60</sub>F<sub>48</sub> interface as a conventional semiconductor hetero interface then this quantity would be characteristic for the interface and hence constant. However, for a weakly interacting molecule such as C<sub>60</sub>F<sub>48</sub>  $\Delta_0$  is determined by the difference between the electron affinity of the molecule and the ionization potential of diamond. The latter in turn depends on the quality of the hydrogen termination which is operational in lowering the ionization potential of diamond to values low enough to make transfer doping possible in the first place. Hence,  $\Delta_0$  can vary even for the same acceptor species and the value determined here for C<sub>60</sub>F<sub>48</sub>,  $\Delta_0 = -0.6 \text{ eV}$ , may vary from case to case.

The final ingredient that enters into the doping efficiency is the Fermi level position in diamond relative to the VBM because the activation energy for electron transfer that enters the Fermi-Dirac statistics equals  $E_a = E_{\text{LUMO}} - E_F$ . This quantity changes as well with doping because the accumulation of positive charge in the subsurface region of diamond induces an upward band bending that also depends on the hole concentration  $p$ . The upward band bending  $w(p) = E_F - E_{\text{VBM}}$  was determined here and amounts to a maximum of 0.74 eV.

From this and previous band bending measurements an empiric functional form for  $w(p)$  has been derived. Together with the other characteristic quantities  $\Delta_0$  and  $C_{\square}$  they have placed us in a position to calculate the doping efficiency, i.e., the ratio of doping to non-doping C<sub>60</sub>F<sub>48</sub> molecules as a function of coverage. As expected, the doping efficiency drops precipitously when the activation energy turns positive, i.e., when the initial negative value of  $\Delta_0$  is compensated by the opposing values of  $w(p)$  and  $\Delta\Phi(p)$ . And that point therefore also determines the maximum achievable hole concentrations and hence surface conductivity. The fact that  $\Delta_0$  is initially negative prevents a freeze-out of carriers at low temperatures. From our analysis it is expected that the same high carrier concentrations of about  $10^{13} \text{ cm}^{-2}$  can be achieved at low temperatures as at room temperature. This is of importance for any planned investigation of the quantization of the 2D hole gas in diamond.

Beyond giving a complete and quantitative picture of the transfer doping of C<sub>60</sub>F<sub>48</sub> on diamond, our work may also serve as a guide for similar donor acceptor systems involving organic molecules and bulk semiconductors because we have considered aside from the effect of quantization of the hole gas all relevant aspects that are operational in such a system.

## ACKNOWLEDGMENTS

We acknowledge financial support from the Australian Research Council DP0879827. Measurements were performed at the Soft X-ray Beamline of the Australian Synchrotron.

- <sup>1</sup>J. B. Cui, J. Ristein, and L. Ley, *Phys. Rev. Lett.* **81**, 429 (1998).
- <sup>2</sup>F. Maier, M. Riedel, B. Mantel, J. Ristein, and L. Ley, *Phys. Rev. Lett.* **85**, 3472 (2000).
- <sup>3</sup>P. Strobel, M. Riedel, J. Ristein, and L. Ley, *Nature (London)* **430**, 439 (2004).
- <sup>4</sup>P. Strobel, M. Riedel, J. Ristein, L. Ley, and O. Boltalina, *Diamond Relat. Mater.* **14**, 451 (2005).
- <sup>5</sup>C. Jin, R. L. Hettich, R. N. Compton, A. Tuinman, A. Derecskei-Kovacs, D. S. Marynick, and B. I. Dunlap, *Phys. Rev. Lett.* **73**, 2821 (1994).
- <sup>6</sup>R. S. Sussman, *CVD Diamond for Electronic Devices and Sensors* (Wiley, New York, 2008), Chap. 4.
- <sup>7</sup>C. E. Nebel, C. Sauerer, F. Ertl, M. Stutzmann, C. F. O. Graeff, P. Bergonzo, O. A. Williams, and R. Jackman, *Appl. Phys. Lett.* **79**, 4541 (2001).
- <sup>8</sup>K. Hayashi, S. Yamanaka, H. Watanabe, T. Sekiguchi, H. Okushi, and K. Kajimura, *J. Appl. Phys.* **81**, 744 (1997).
- <sup>9</sup>M. T. Edmonds, C. I. Pakes, and L. Ley, *Phys. Rev. B* **81**, 085314 (2010).
- <sup>10</sup>H. Kawarada, M. Aoki, and M. Ito, *Appl. Phys. Lett.* **65**, 1563 (1994).
- <sup>11</sup>H. Kawarada, Y. Araki, T. Sakai, and T. Ogawa, *Phys. Status Solidi A* **185**, 79 (2001).
- <sup>12</sup>As quoted by supplier Element6; [www.e6cvd.com](http://www.e6cvd.com).
- <sup>13</sup>K. J. Rietwyk, M. Wanke, H. M. Vulling, M. T. Edmonds, P. L. Sharp, Y. Smets, Q.-H. Wu, A. Tadich, S. Rubanov, P. J. Moriarty, L. Ley, and C. I. Pakes, *Phys. Rev. B* **84**, 035404 (2011).
- <sup>14</sup>D. A. Shirley, *Phys. Rev. B* **5**, 4709 (1972).
- <sup>15</sup>R. Graupner, F. Maier, J. Ristein, L. Ley, and C. Jung, *Phys. Rev. B* **57**, 12397 (1998).
- <sup>16</sup>F. Maier, J. Ristein, and L. Ley, *Phys. Rev. B* **64**, 165411 (2001).
- <sup>17</sup>M. T. Edmonds, C. I. Pakes, S. Mammadov, W. Zhang, A. Tadich, J. Ristein, and L. Ley, *Appl. Phys. Lett.* **98**, 102101 (2011).
- <sup>18</sup>K. J. Rietwyk *et al.*, "High resolution core level spectroscopy of hydrogen-terminated diamond" (unpublished).
- <sup>19</sup>M. T. Edmonds, C. I. Pakes, S. Mammadov, W. Zhang, A. Tadich, J. Ristein, and L. Ley, *Phys. Status Solidi A* **208**, 2062 (2011).
- <sup>20</sup>Y. Gao, *Mater. Sci. Eng. R.* **68**, 39 (2010).
- <sup>21</sup>S. Braun, W. R. Salaneck, and M. Fahlman, *Adv. Mater.* **21**, 1450 (2009).

<sup>22</sup>J. Ristein, *Diamond Relat. Mater.* **13**, 808 (2004).

<sup>23</sup>R. Mitsumoto, T. Araki, E. Ito, Y. Ouchi, K. Seki, K. Kikuchi, Y. Achiba, H. Kurosaki, T. Sonoda, H. Kobayashi, O. Boltalina, V. Pavlovich, L. Sidorov, Y. Hattori, N. Liu, S. Yajima, S. Kawasaki, F. Okino, and H. Touhara, *J. Phys. Chem. A* **102**, 552 (1998).

<sup>24</sup>J. D. Wright, *Molecular Crystals* (Cambridge University Press, Cambridge, England, 1987).

<sup>25</sup>R. Mitsumoto, K. Seki, T. Araki, E. Ito, Y. Ouchi, Y. Achiba, K. Kikuchi, S. Yajima, S. Kawasaki, F. Okino, H. Touhara, H. Kurosaki, T. Sonoda, and H. Kobayashi, *J. Electron Spectrosc. Relat. Phenom.* **78**, 453 (1996).